

Fast frequency-resolved terahertz imaging

Takashi Yasuda, Yoichi Kawada, Haruyoshi Toyoda, Atsushi Nakanishi, Koichiro Akiyama, and Hironori Takahashi

Central Research Laboratory, Hamamatsu Photonics K.K., 5000 Hirakuchi, Hamakita-ku, Hamamatsu City 434-8601, Japan

(Received 31 August 2010; accepted 8 March 2011; published online 31 March 2011)

We propose a fast, frequency-resolved, real-time, terahertz imaging method. With our method, images at two specific terahertz frequencies can be acquired in 1 min. Three kinds of drugs (L-histidine, maltose, and CBZ3), which have absorption peaks in the terahertz region, were distinguished in 3 min by using our method. This technique can be used in industrial applications, such as nondestructive testing. © 2011 American Institute of Physics. [doi:10.1063/1.3571303]

I. INTRODUCTION

Terahertz (THz) electromagnetic waves (0.1–10 THz) have many interesting characteristics, such as high transmittance, noninvasiveness, sensitivity to intermolecular forces, and low scattering. THz techniques, such as spectroscopy^{1–3} and imaging,^{4–6} are very attractive for numerous scientific and industrial applications.

The THz imaging, which is based on the high transmittance of THz waves in nonmetallic materials, is expected to be an important tool for security and nondestructive testing. We successfully achieved real-time THz imaging.⁷ In that study, the obtained images included all frequency components of the THz pulse, and the spatial resolution deteriorated at lower frequencies. In addition, two different objects could not be distinguished in the THz image.

Frequency-resolved imaging provides images at specific frequencies. This technique can improve the spatial resolution if images with high-frequency components are selected. It is also possible to discriminate a particular object by choosing an image obtained at an absorption-peak frequency. Two types of frequency-resolved imaging have been demonstrated: the raster scanning method^{8–11} and the two-dimensional (2D) electro-optical (EO) sampling method.^{12–14} In the raster scanning method, the sample needs to be moved. On the other hand, the 2D EO sampling method can obtain a 2D image without moving the sample. One problem with this method, however, is the long data analysis time required because a large amount of 2D imaging data must be processed. This is a critical issue that must be overcome in order to use the technique in industrial applications.

The 2D EO sampling method uses the following procedures: (1) 2D THz waveform data are required. That is, THz images are acquired for all sampling points by scanning a time-delay line. (2) The time domain information at each pixel of the obtained THz images is converted to frequency information by Fourier transformation. (3) A frequency-resolved image is reconstructed by collecting the amplitude information for a specific frequency at all pixels.

In this paper, we propose a fast frequency-resolved THz imaging technique in which we focus on the integration process. The time required for the integration process is equivalent to a waiting time. During the waiting time, we can convert

the time information to frequency information by using a sin-cos conversion, which allows a specific-frequency-resolved image to be acquired at high speed.

II. SYSTEM CONFIGURATION

Figure 1 schematically shows the design of our 2D THz imaging system.⁷ The regenerative amplifier Ti:Sapphire laser system has a repetition rate of 1 kHz, a pulse duration of 50 fs, an output energy of 2.5 mJ, and a center wavelength of 800 nm. The THz emitter and detector are 1 mm-thick (110) ZnTe crystals. The THz pulse generated in the emitter is incident on the sample and is then imaged onto a detector by two lenses. When the THz and probe pulses are incident on the detector simultaneously, the probe beam is modulated by THz-induced birefringence. The modulation distribution is proportional to the intensity of the THz image of the sample and is detected by a 2D CMOS camera [Intelligent Vision Sensor: IVS, Hamamatsu C82150–50, 232 × 232 pixel, 1000 fps (Ref. 15)] using a dynamic subtraction technique.^{16,17} In this technique, the CMOS camera is synchronized with the laser repetition rate, and the THz image is modulated by a chopper at half of the laser repetition rate. We acquire THz-on and THz-off frames alternately on the CMOS camera and subtract these frames. Finally, we obtain a THz image with good signal-to-noise ratio (10:1) (Ref. 7) by integrating these subtracted frames.

III. ALGORITHM

To obtain a specific-frequency image at high speed, we propose the following methods. Details of the processing flow, shown in Fig. 2, are described in the following.

1. The 2D THz time waveform data are obtained by acquiring a 2D THz image every sampling period by scanning the time-delay line.

2. In the waiting time at every sampling period for the integration frames, we multiply the subtracted and integrated frames using Eq. (1) (sin-cos conversion process) and store

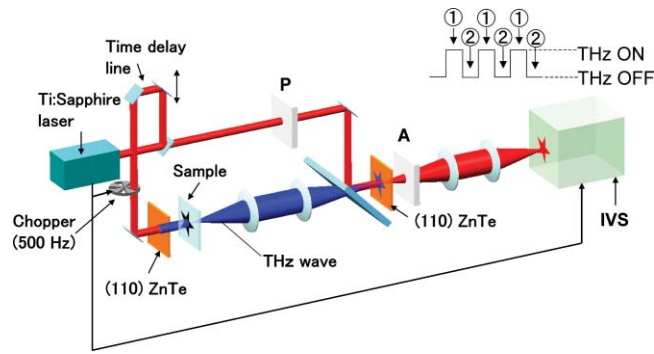


FIG. 1. (Color online) Experimental setup.

the calculated results,

$$X_F = \sum_{k=0}^{N-1} x_k \left(\cos \frac{2\pi nk}{N} - j \sin \frac{2\pi nk}{N} \right), \quad (1)$$

where X_F is the image at frequency F (THz), N is the number of sampling points, x_k is the k th THz image data, and n is the order of the frequency ($= F/\Delta f$). The specific-frequency images are obtained simultaneously when the measurement is completed.

3. After the measurement, we can obtain frequency-resolved THz images by integrating the stored data following Eq. (1).

Providing that the processing time of the calculation is short enough, two or more images can be obtained by preparing frequency tables. In this algorithm, the measurement and analysis times are limited by the number of sampling points and integration frames. When integration is performed over 50 frames with 512 sampling points, we can acquire two frequency-resolved THz images in 1 min.

IV. EXPERIMENTAL RESULTS

We experimentally evaluated the validity of our algorithm by comparing spectra obtained with our method and the conventional method. First, THz images were acquired in the frequency range 0–5 THz at intervals of 0.33 THz, using

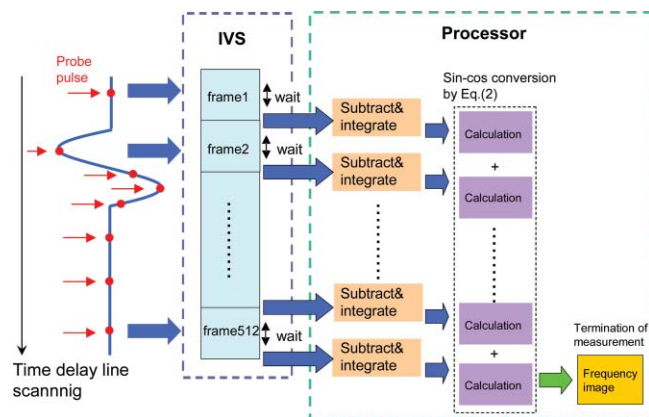


FIG. 2. (Color online) Flow chart of fast frequency-resolved terahertz image technique.

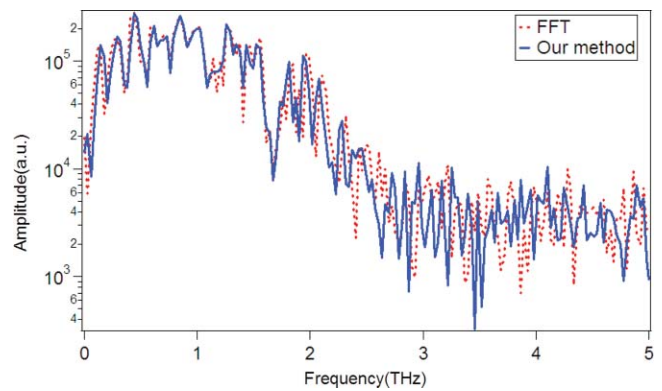


FIG. 3. (Color online) Comparison between conventional FFT-based method and our method.

the two methods. Then, spectra were extracted from the center pixels of these THz images. The results are shown in Fig. 3. The dashed line (red) is the spectrum acquired using the conventional method, and the solid line (blue) is the spectrum acquired using our algorithm. The noise in the spectra was likely due to water vapor in the air. The difference between the red and blue lines at high frequencies is thought to be caused by changes in the environment, such as humidity. On the whole, the two results are in good agreement, showing the validity of our algorithm.

We acquired two frequency images of two tablets, which could be distinguished using our method. One was a 100% polyethylene tablet, and the other consisted of 50% polyethylene and 50% lactose (lactose tablet). These tablets were 8 mm in diameter and 1.5 mm thick and were fixed on a sample holder with a $\varphi 10$ mm clear aperture. The upper tablet is the polyethylene tablet, and the lower one is the lactose tablet. We acquired an image at 1.37 THz [lactose absorption peak; see absorption spectrum acquired by THz time domain spectroscopy (THz TDS) shown in Fig. 4] and an image at 1.5 THz (no lactose absorption) in 1 min.

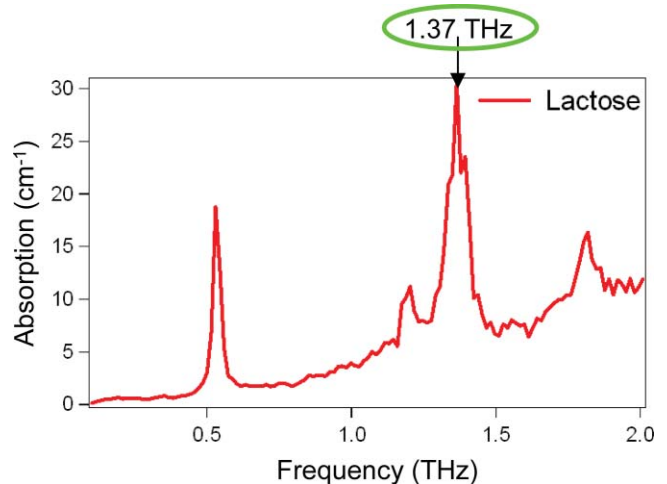


FIG. 4. (Color online) Absorption spectrum of lactose acquired by THz TDS.

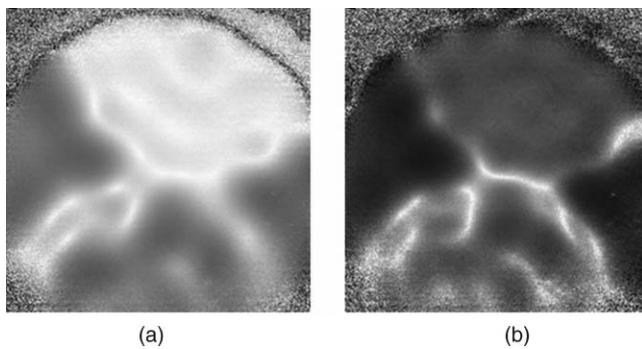


FIG. 5. Contrast images of lactose and polyethylene obtained at (a) 1.37 THz and (b) 1.5 THz.

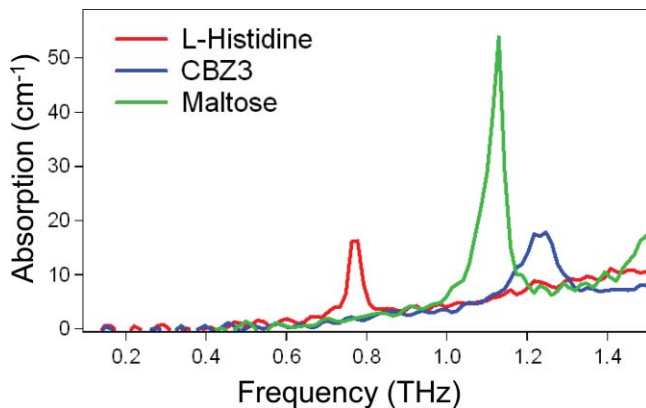


FIG. 6. (Color online) Absorption spectra of L-histidine, maltose, and CBZ3 acquired by THz TDS.

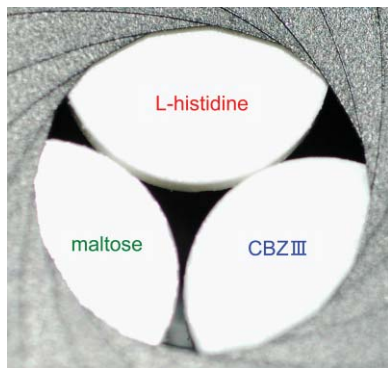


FIG. 7. (Color online) Sample tablets (L-histidine, maltose, and CBZ3) were fixed on an aperture with 10 mm diameter.

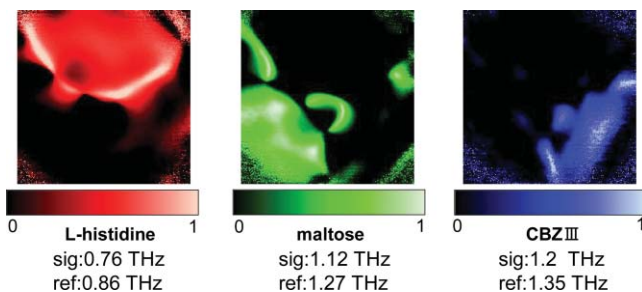


FIG. 8. (Color online) Contrast images for 0.76, 1.12, and 1.2 THz, which are absorption peak frequencies.

We define a contrast image as

$$\text{contrast} = \frac{\text{ref} - \text{sig}}{\text{ref} + \text{sig}}, \quad (2)$$

where sig is the signal image of the sample, obtained at the absorption peak frequency, and ref is a reference image obtained at the same frequency with no sample. A contrast image obtained using a 1.37 THz signal image (sig) and a 1.37 THz reference image (ref) is shown in Fig. 5. In Fig. 5(a), the lactose image is clearly separated, showing that we can distinguish between lactose and polyethylene. A contrast image obtained using 1.5 THz is shown in Fig. 5(b); the two tablets are indistinguishable.

Next, we measured three kinds of chemical tablets: maltose, a sugar; CBZ3, a treatment of epilepsy; and L-histidine, an essential amino acid. These absorption spectra acquired by THz TDS are shown in Fig. 6. Each tablet was fixed on an aperture (10 mm diameter, Fig. 7). We acquired absorption-peak images at 1.12, 1.2, and 0.76 THz.

In the result shown in Fig. 5, we adopted the frequency image obtained without a sample as a reference image. However, this method is not practical. Instead, here we used an image at a frequency of 0.1 or 0.15 THz from each absorption peak as the reference image. This allowed the contrast image to be acquired rapidly (in 1 min).

The total measurement time for the three images was 3 min. The contrast images between the absorption-peak and reference frequencies are shown in Fig. 8 for each tablet. The three tablets are clearly distinguished.

V. CONCLUSIONS

We proposed a new processing method to obtain specific-frequency THz images at high speed. With this method, two images at different frequencies were acquired in 1 min. Also, three kinds of drugs (L-histidine, maltose, and CBZ3) were distinguished by employing contrast images. This technique can be used in industrial applications, such as nondestructive testing.

ACKNOWLEDGMENTS

The authors thank T. Hiruma, A. Hiruma, Y. Suzuki, T. Hara, and S. Aoshima for their encouragement, and M. Fujimoto and H. Ito for their helpful discussions.

- ¹D. Grischkowsky, S. Keiding, M. Van Exter, and Ch. Fittinger, *J. Opt. Soc. Am. B* **7**, 2006 (1990).
- ²H. Harde and D. Grischkowsky, *J. Opt. Soc. Am. B* **8**, 1642 (1991).
- ³M. C. Nuss, K. W. Goossen, J. P. Gordon, P. M. Mankiewich, M. L. O'Malley, and M. Bhushan, *J. Appl. Phys.* **70**, 2238 (1991).
- ⁴B. B. Huss and M. C. Nuss, *Opt. Lett.* **20**, 1716 (1995).
- ⁵D. M. Mittlemam, R. H. Jacobsen, and M. C. Nuss, *IEEE J. Sel. Top. Quantum Electron.* **2**, 679 (1996).
- ⁶Q. Wu, T. D. Hewitt, and X.-C. Zhang, *Appl. Phys. Lett.* **69**, 1026 (1996).
- ⁷T. Yasuda, Y. Kawada, H. Toyoda, and H. Takahashi, *Opt. Express* **15**, 15583 (2007).
- ⁸K. Kawase, Y. Ogawa, Y. Watanabe, and H. Inoue, *Opt. Express* **11**, 2549 (2003).
- ⁹Y. Watanabe, K. Kawase, T. Ikari, H. Ito, Y. Ishikawa, and H. Minamide, *Opt. Commun.* **234**, 125 (2004).
- ¹⁰Y. C. Shen, T. Lo, P. F. Taday, B. E. Cole, W. R. Tribe, and M. C. Kemp, *Appl. Phys. Lett.* **86**, 241116 (2005).

- ¹¹H. Hoshina, A. Hayashi, N. Miyoshi, F. Miyamaru, and C. Otani, *Appl. Phys. Lett.* **94**, 123901 (2009).
- ¹²M. Usami, M. Yamashita, K. Fukushima, C. Otani, and K. Kawase, *Appl. Phys. Lett.* **86**, 141109 (2005).
- ¹³H. Zhong, A. Redo-Sanchez, and X.-C. Zhang, *Opt. Express* **14**, 9130 (2006).
- ¹⁴Y. C. Shen, L. Gan, M. Stringer, A. Burnett, K. Tych, H. Shen, J. E. Cunningham, E. P. J. Parrott, J. A. Zeitler, L. F. Gladden, E. H. Linfield, and A. G. Davies, *Appl. Phys. Lett.* **95**, 231112 (2009).
- ¹⁵Y. Sugiyama, M. Takumi, H. Toyoda, N. Mukozaka, A. Ihori, T. Kurashina, Y. Nakamura, T. Tonbe, and S. Mizuno, *IEEE J. Solid-State Circuits* **40**, 2816 (2005).
- ¹⁶Z. Jiang, X. G. Xu, and X.-C. Zhang, *Appl. Opt.* **39**, 2982 (2000).
- ¹⁷F. Miyamaru, T. Yonera, M. Tani, and M. Hangyo, *Jpn. J. Appl. Phys.* **43**, L489 (2004).